

## The Silicon Vertex Detector of the Belle II Experiment

K. Lautenbach,<sup>a,\*</sup> K. Adamczyk,<sup>b</sup> L. Aggarwal,<sup>c</sup> H. Aihara,<sup>d</sup> T. Aziz,<sup>e</sup> S. Bacher,<sup>b</sup> S. Bahinipati,<sup>f</sup> G. Batignani,<sup>i,j</sup> J. Baudot,<sup>g</sup> P. K. Behera,<sup>h</sup> S. Bettarini,<sup>i,j</sup> T. Bilka,<sup>k</sup> A. Bozek,<sup>b</sup> F. Buchsteiner,<sup>l</sup> G. Casarosa,<sup>i,j</sup> L. Corona,<sup>i,j</sup> T. Czank,<sup>q</sup> S. B. Das,<sup>l</sup> G. Dujany,<sup>g</sup> C. Finck,<sup>g</sup> F. Forti,<sup>i,j</sup> M. Friedl,<sup>l</sup> A. Gabrielli,<sup>m,n</sup> E. Ganiev,<sup>B, m,n</sup> B. Gobbo,<sup>n</sup> S. Halder,<sup>e</sup> K. Hara,<sup>o,p</sup> S. Hazra,<sup>e</sup> T. Higuchi,<sup>q</sup> C. Irmeler,<sup>l</sup> A. Ishikawa,<sup>o,p</sup> H. B. Jeon,<sup>r</sup> Y. Jin,<sup>m,n</sup> M. Kaleta,<sup>b</sup> A. B. Kaliyar,<sup>e</sup> J. Kandra,<sup>k</sup> K. H. Kang,<sup>q</sup> P. Kapusta,<sup>b</sup> P. Kodyš,<sup>k</sup> T. Kohriki,<sup>o</sup> M. Kumar,<sup>t</sup> R. Kumar,<sup>u</sup> C. La Licata,<sup>q</sup> K. Lalwani,<sup>t</sup> R. Leboucher,<sup>a</sup> S. C. Lee,<sup>r</sup> J. Libby,<sup>h</sup> L. Martel,<sup>g</sup> L. Massaccesi,<sup>i,j</sup> S. N. Mayekar,<sup>e</sup> G. B. Mohanty,<sup>e</sup> T. Morii,<sup>q</sup> K. R. Nakamura,<sup>o,p</sup> Z. Natkaniec,<sup>b</sup> Y. Onuki,<sup>d</sup> W. Ostrowicz,<sup>b</sup> A. Paladino,<sup>A, i,j</sup> E. Paoloni,<sup>i,j</sup> H. Park,<sup>r</sup> L. Polat,<sup>a</sup> K. K. Rao,<sup>e</sup> I. Ripp-Baudot,<sup>g</sup> G. Rizzo,<sup>i,j</sup> D. Sahoo,<sup>e</sup> C. Schwanda,<sup>l</sup> J. Serrano,<sup>a</sup> J. Suzuki,<sup>o</sup> S. Tanaka,<sup>o,p</sup> H. Tanigawa,<sup>d</sup> R. Thalmeier,<sup>l</sup> R. Tiwary,<sup>e</sup> T. Tsuboyama,<sup>o,p</sup> Y. Uematsu,<sup>d</sup> L. Vitale,<sup>m,n</sup> K. Wan,<sup>d</sup> Z. Wang,<sup>d</sup> J. Webb,<sup>s</sup> O. Werbycka,<sup>n</sup> J. Wiechczynski,<sup>b</sup> H. Yin<sup>l</sup> and F. Tenchini<sup>i,j</sup>

<sup>a</sup>School of Physics, University of Melbourne, Melbourne, Victoria 3010, Australia

<sup>l</sup>Institute of High Energy Physics, Austrian Academy of Sciences, 1050 Vienna, Austria

<sup>k</sup>Faculty of Mathematics and Physics, Charles University, 121 16 Prague, Czech Republic

<sup>a</sup>Aix Marseille Université, CNRS/IN2P3, CPPM, 13288 Marseille, France

<sup>g</sup>IPHC, UMR 7178, Université de Strasbourg, CNRS, 67037 Strasbourg, France

<sup>f</sup>Indian Institute of Technology Bhubaneswar, Satya Nagar, India

<sup>h</sup>Indian Institute of Technology Madras, Chennai 600036, India

<sup>d</sup>Malaviya National Institute of Technology Jaipur, Jaipur 302017, India

<sup>u</sup>Punjab Agricultural University, Ludhiana 141004, India

<sup>c</sup>Punjab University, Chandigarh 160014, India

<sup>e</sup>Tata Institute of Fundamental Research, Mumbai 400005, India

<sup>i</sup>Dipartimento di Fisica, Università di Pisa, I-56127 Pisa, Italy, <sup>A</sup>presently at INFN Sezione di Bologna, I-40127 Bologna, Italy

<sup>j</sup>INFN Sezione di Pisa, I-56127 Pisa, Italy

<sup>m</sup>Dipartimento di Fisica, Università di Trieste, I-34127 Trieste, Italy, <sup>B</sup>presently at DESY, Hamburg 22761, Germany

<sup>n</sup>INFN Sezione di Trieste, I-34127 Trieste, Italy

<sup>p</sup>The Graduate University for Advanced Studies (SOKENDAI), Hayama 240-0193, Japan

<sup>q</sup>Kavli Institute for the Physics and Mathematics of the Universe (WPI), University of Tokyo, Kashiwa 277-8583, Japan

\*Speaker

<sup>d</sup>Department of Physics, University of Tokyo, Tokyo 113-0033, Japan

<sup>o</sup>High Energy Accelerator Research Organization (KEK), Tsukuba 305-0801, Japan

<sup>r</sup>Department of Physics, Kyungpook National University, Daegu 41566, Korea

<sup>b</sup>H. Niewodniczanski Institute of Nuclear Physics, Krakow 31-342, Poland

E-mail: [lautenbach@cppm.in2p3.fr](mailto:lautenbach@cppm.in2p3.fr)

The Belle II experiment started taking data at the SuperKEKB collider in spring 2019. As part of the inner tracker system, the silicon vertex detector (SVD) has been operating reliably. It provided good data quality, a good signal-to-noise ratio, an excellent hit efficiency greater than 99% and precise spatial resolution, which result in good tracking efficiency. The current occupancy, which is dominated by beam-background hits, is around 0.5% in the innermost layer and does so far not cause problems to the SVD data reconstruction. Due to the estimated increase in occupancy at higher luminosity in the next years, specific strategies aiming to preserve the tracking performance were developed and tested on data. Strip noise, sensor currents and depletion voltages have been measured to check for the first effects of radiation damage. So far no harmful impact on the detector performance has been observed. Extrapolations for the next years do not imply upcoming problems, although these background estimates are still affected by large uncertainties. No damage due to beam losses or sudden intense radiation bursts were detected.

41st International Conference on High Energy physics - ICHEP2022  
6-13 July, 2022  
Bologna, Italy

## 1. Overview

The Belle II experiment [1], which is located at the SuperKEKB [2] collider, mostly operates at the centre-of-mass energy of the  $\Upsilon(4S)$  resonance and aims at probing new physics beyond the Standard Model through precision measurements on large samples of  $B$  mesons,  $\tau$  and charm decays. Due to its asymmetric beam energies of 7 and 4 GeV, for the electron and positron beams respectively, one can exploit the boosted  $B$  meson system to measure time dependent  $CP$ -violation. The world record instantaneous luminosity of  $4.7 \times 10^{34} \text{ cm}^{-2} \text{ s}^{-1}$  was measured in December 2021, the final peak luminosity is expected to be  $6 \times 10^{35} \text{ cm}^{-2} \text{ s}^{-1}$ . Belle II already collected more than  $420 \text{ fb}^{-1}$ , the final target is to accumulate up to  $50 \text{ ab}^{-1}$ , which would result in a 50 times larger data set than the predecessor Belle. Belle II needs to provide similar or better performance in a harsher beam background environment. Moreover, it must achieve better vertex resolution to compensate for the reduced boost  $\beta\gamma$  from 0.45 at KEKB to 0.28 at SuperKEKB, and so ensure similar or better time resolution. As a precision frontier experiment, Belle II is required to accumulate a high statistics data set, feature a precise vertexing, excellent track reconstruction and energy-loss measurement, as well as particle identification, also for low momentum tracks. The innermost tracking device, the vertex detector (VXD), is composed of two inner layers of DEPFET pixel sensors - the Pixel Detector (PXD) - and four layers of double-sided silicon strip detectors (DSSD), which compose the silicon vertex detector. Due to the high luminosity and its location close to the beam pipe 14, (39) mm, the PXD (SVD) has to cope with hit rates of 20 (3) MHz/cm<sup>2</sup> and requires a radiation hardness of 2 (0.2) Mrad/year. In this proceeding, we describe the SVD (Sec. 2), its operational experience and performance (Sec. 3), beam-background and occupancy limits (Sec. 4) and radiation-damage effects (Sec. 5).

## 2. The Belle II Silicon Vertex Detector

The SVD is composed of 172 DSSD sensors, which are arranged in four layers, the innermost (L3) at 39 mm and the outermost (L6) at 135 mm. From L3 to L6 the number of sensors per ladder increments by one starting with two sensors on L3. The average material budget per layer is 0.7% of the radiation length  $X_0$ . For radiation monitoring it features diamond sensors installed on the beam pipe, which can also be used to trigger a beam abort [3], in case sudden radiation spikes are detected. Each sensor is based on an N-type bulk between 300-320  $\mu\text{m}$  thick, equipped with implanted P- and N-doped sensitive strips on opposite sides. Readout and floating (not readout) strips are alternated on top of a dielectric  $\text{SiO}_2$  layer. The implanted strips below are AC coupled with the readout strips. The u/P side strips, orthogonal to the beam axis, measure the  $r\phi$ -direction and the v/N side provides information on the z-coordinate along the beam line. Three different geometrical shapes are used; a small rectangular one for layer 3, a large rectangular one for layers 4, 5 and 6 and a slanted trapezoidal type in the forward region. The APV25 [4] front-end electronic chips collect the signal and provide analog readout. Each chip features 128 channels with a fast 50 ns shaping time and radiation hardness up to 100 Mrad. Six subsequent analog samplings reconstruct the signal waveform with a 32 MHz clock, running asynchronous to the bunch crossing frequency, which is about eight times higher. The chips are thinned to 100  $\mu\text{m}$  to minimize the material budget and stainless steel pipes for bi-phase  $\text{CO}_2$  cooling at  $-20^\circ$  are located on one side only. The SVD

fulfills three main roles: it extrapolates the tracks to the PXD; it defines regions of interest for data reduction of the PXD data stream and it provides standalone tracking and particle identification via the measurement of ionisation energy loss. A detailed description of the SVD layout, readout and assembly can be found in [5].

### 3. Operation and performance

The SVD has been operating smoothly with no major issues since its installation in 2019. So far, the total fraction of masked strips is less than 1% and only one APV25 chip out of 1748 was temporarily disabled. Temperature and calibration constants are evolving in the expected ranges due to radiation damage and the hit efficiency is above 99% for all sensors. The signal charge normalised to the traversed sensor thickness, shown in Figure 1 (a), is found to be in good agreement with expectations and similar in all sensors. The charge matches with the expected MIP value for the u/P side when accounting for the APV25 calibration uncertainty, while on v/N side a signal loss of 10%-30% is observed due to the larger pitch and floating strips. A very good signal-to-noise (SNR) ratio is measured in all sensors, with most probable value ranging between 13-30; an example is shown in Figure 1 (b). For good vertexing and track reconstruction, an excellent resolution on the

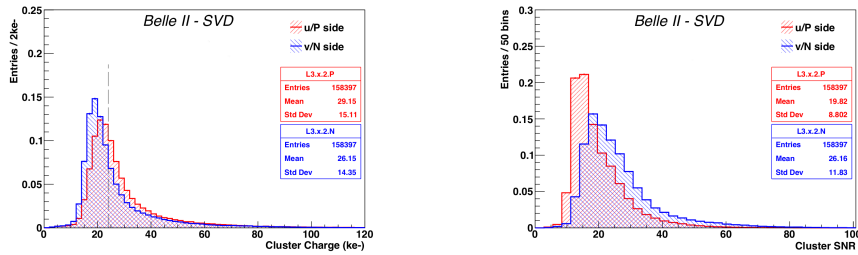


**Figure 1:** Cluster charge normalised by the track path length and scaled to the sensor thickness (left) and signal-to-noise ratio (SNR) for the backward sensors of layer 3, averaged on all ladders (right) for the u/P and v/N side in red and blue respectively. The dashed grey line in the left plot corresponds to 24 the expected most probable value (MPV) for a minimal ionising particle (MIP).

cluster position is crucial. Results on the resolution are in fair agreement with expectations from the pitch, giving 9 (11)  $\mu\text{m}$  for layer 3 (4, 5 and 6) u/P side and 20 (25)  $\mu\text{m}$  for layer 3 (4, 5 and 6) v/N side. The underlying measurement is performed on  $e^+e^- \rightarrow \mu^+\mu^-$  events by estimating the residual of the cluster position with respect to the unbiased track extrapolation after subtracting the effect of the error on the track intercept. Optimal hit-time resolution of less than 2.9 (2.4) ns for u/P (v/N) side is achieved on the SVD time, which is calibrated with respect to the event time provided by the Belle II central drift chamber (CDC). Due to this excellent time resolution, around 50% of the background hits could be rejected while preserving more than 99% of the signal, as a study on data has shown. This selection is currently not implemented, but will help against larger background levels expected at higher luminosities.

### 4. Beam-background and occupancy limit

An increase in beam-background hits can degrade the tracking performance and causes radiation damage. The higher occupancy, which results from a beam-background increase, leads to a

larger number of clusters which can be wrongly associated to tracks or create fake tracks in the reconstruction. For layer 3 the current occupancy limit is expected to be around 3%, which could be approximately doubled by exploiting the information on the hit time to reject background hits. At the present luminosity the average hit occupancy in layer 3 is below 0.5% and it reaches 3% at the design luminosity of  $6 \times 10^{35} \text{ cm}^{-2} \text{ s}^{-1}$  according to beam-background projections, which are based on scaling the simulation with a data-simulation ratio. This extrapolation is affected by large uncertainties due to the assumption of optimal collimator settings and the missing contribution of the injection background not yet simulated. Since the safety factor is relatively small a proposal for a vertex upgrade has been made and the technology assessment is currently ongoing. The integrated dose on the SVD sensors is estimated from the correlation between the measured occupancy and the dose rate measured in the diamond sensors and is based on several assumptions that result in an uncertainty of about 50%. The most exposed mid plane of layer 3 collected less than 20 krad dose during the summer 2022 run period. The total integrated dose on the SVD up to the long shutdown in summer 2022 corresponds to a 1-MeV neutron equivalent fluence of  $1.6 \times 10^{11} \text{ n}_{\text{eq}}/\text{cm}^2$ , assuming a ratio of  $2.3 \times 10^9 \text{ n}_{\text{eq}}/\text{cm}^2/\text{krad}$  between dose and neutron equivalent from simulation studies.

## 5. Radiation damage effects

Radiation damage has already produced observable effects, but these do not degrade the performance. The increase of leakage current, due to the sensor-bulk damage caused by non-ionising energy loss (NIEL) [6], is proportional to the 1-MeV neutron equivalent fluence, which itself is proportional to the integrated dose. This results in a linear correlation between the leakage current and the integrated dose, which is observed on all sensors with slopes between 2 to 5  $\mu\text{A}/\text{cm}^2/\text{Mrad}$ . This result is the same order of magnitude as the effect measured by the BaBar experiment of 1  $\mu\text{A}/\text{cm}^2/\text{Mrad}$  at 20°C [7]. The noise increase is currently dominated by the strip capacitance and the leakage current contribution is highly suppressed by the short shaping time of the APV25. With the measured increase of the leakage current with dose, we expect to observe a significant deterioration of the noise and SNR due to leakage current only at about 6 Mrad. Thus the irradiation is not expected to degrade the performance even after 10 years at design luminosity, considering the current background extrapolations of about 0.2 Mrad/yr in the innermost SVD layer, that are anyway still affected by large uncertainties. The radiation damage is also visible in a general increase of strip noise of 10% (30%) on n/V (u/P) side, due to a surface effect induced by radiation on the sensors. This non-linear increase is related to fixed oxide charges in the SiO<sub>2</sub> layer increasing the inter-strip capacitance, which is expected to saturate, as it has already been observed in the v/N side. The saturation level has been reached also in the layer 3 u/P side, while in the outer layers of u/P it is still rising. No degradation of the SVD performance has been observed due to the noise increase. Finally, non-ionising energy loss causes sensor bulk damage that can result in a change of the effective doping and therefore of the depletion voltage. This effect can be monitored by measuring the v/N side noise as a function of the applied bias voltage, since N-type strips are completely insulated when the N-type bulk is fully depleted, causing also the strip noise to drop. Hence, the voltage for which the strip noise on the v/N-side reaches its minimum allows a measurement of the depletion voltage, which is shown to be constant and no changes are observed

due to radiation, as expected for a low integrated 1-MeV neutron equivalent fluence accumulated so far.

## Conclusions and Outlooks

The Belle II SVD has been fully functional since March 2019. It has run with excellent and stable performance in agreement with expectations. First effects of radiation damage were observed at the expected level. There is no negative impact on the performance and the system is ready to cope with higher beam-backgrounds due to future increases to luminosity.

## Acknowledgements

This project has received funding from the European Union’s Horizon 2020 research and innovation programme under the Marie Skłodowska-Curie grant agreements No 644294 and 822070 and ERC grant agreement No 819127. This work is supported by MEXT, WPI, and JSPS (Japan); ARC (Australia); BMBWF (Austria); MSMT (Czechia); CNRS/IN2P3 (France); AIDA-2020 (Germany); DAE and DST (India); INFN (Italy); NRF and RSRI (Korea); and MNiSW (Poland).

## References

- [1] T. Abe, et al., Belle II Technical Design Report (2010). [arXiv:1011.0352](https://arxiv.org/abs/1011.0352).
- [2] K. Akai, K. Furukawa, H. Koiso, SuperKEKB Collider, Nucl. Instrum. Meth. A 907 (2018) 188–199. [arXiv:1809.01958](https://arxiv.org/abs/1809.01958), [doi:10.1016/j.nima.2018.08.017](https://doi.org/10.1016/j.nima.2018.08.017).
- [3] S. Bacher, et al., Performance of the diamond-based beam-loss monitor system of Belle II, Nucl. Instrum. Meth. A 997 (2021) 165157. [arXiv:2102.04800](https://arxiv.org/abs/2102.04800), [doi:10.1016/j.nima.2021.165157](https://doi.org/10.1016/j.nima.2021.165157).
- [4] M. J. French, et al., Design and results from the APV25, a deep sub-micron CMOS front-end chip for the CMS tracker, Nucl. Instrum. Meth. A 466 (2001) 359–365. [doi:10.1016/S0168-9002\(01\)00589-7](https://doi.org/10.1016/S0168-9002(01)00589-7).
- [5] F. Forti, The design, construction, operation and performance of the belle ii silicon vertex detector (2022). [doi:10.48550/ARXIV.2201.09824](https://doi.org/10.48550/ARXIV.2201.09824).  
URL <https://arxiv.org/abs/2201.09824>
- [6] G. Lindström, M. Ahmed, et al., Developments for radiation hard silicon detectors by defect engineering—results by the CERN RD48 (ROSE) Collaboration, Nuclear Instruments and Methods in Physics Research Section A: Accelerators, Spectrometers, Detectors and Associated Equipment 465 (1) (2001) 60–69, sPD2000. [doi:https://doi.org/10.1016/S0168-9002\(01\)00347-3](https://doi.org/10.1016/S0168-9002(01)00347-3).
- [7] The BABAR Collaboration, The babar detector: Upgrades, operation and performance (2013). [doi:10.48550/ARXIV.1305.3560](https://doi.org/10.48550/ARXIV.1305.3560).  
URL <https://arxiv.org/abs/1305.3560>